national accelerator laboratory

NAL-73/20-EXP
7200.037

UCLA-1073

pp INTERACTIONS AT 303 GeV/c; TESTS OF SCALING IN SINGLE PARTICLE $\pi^{\pm}$ AND PROTON DISTRIBUTIONS

F. T. Dao, D. Gordon, J. Lach, E. Malamud, and J. Schivell
National Accelerator Laboratory, Batavia, Illinois 60510 USA

and

T. Meyer, R. Poster, P. E. Schlein, and W. E. Slater
University of California, Los Angeles, California 90024 USA

June 1973

Operated by Universities Research Association Inc. Under Contract with the United States Atomic Energy Commission

pp INTERACTIONS AT 303 GeV/c; TESTS OF SCALING IN SINGLE PARTICLE $\pi^{\pm}$ AND PROTON DISTRIBUTIONS

F. T. Dao, D. Gordon, J. Lach, E. Malamud, and J. Schivell
National Accelerator Laboratory, Batavia, Illinois 60510 USA

and

T. Meyer, R. Poster, P. E. Schlein, and W. E. Slater*
University of California, Los Angeles, California 90024 USA

June 1973

This paper is one of a series of several articles concerning proton-proton interactions at 303 GeV/c as observed in the National Accelerator Laboratory-Argonne 30-inch hydrogen bubble chamber.

We present here results of single π^+, π^-, and proton invariant cross-section distributions. These distributions are compared with existing data at higher c.m. energy from the CERN-ISR and at lower c.m. energy from the CERN-PS and the BNL-AGS.

As described in our earlier paper on $\Delta^{++}(1236)$ production,[1] particles which travel backward in the pp center-of-mass have comparatively low momenta in the laboratory and can be measured with conventional film measuring machines and analysis techniques. Such measurements have been performed on all tracks with laboratory momenta $P_{lab} \leq 1.4$ GeV/c. Since protons with this momentum have 1.4 x minimum ionization, pions and protons are distinguished with good reliability by their ionization. From the number of observed events involving K_S^o emission as well as direct ionization information, we estimate that the amount of $K^{\pm}$ contamination in the π-p sample is ~2-3%, which we ignore for the purposes of the present paper.

Of the 1750 events in the fiducial volume used for the present investigation, 806 events were found which have a single proton with $P_{lab} < 1.4$ GeV/c. To illustrate the kinematically accepted region and the overall qualitative properties of the data, the c.m. distribution of these protons in the variables $x = 2P_{\parallel}/\sqrt{s}$ and the transverse momentum P_t^2 is shown in Fig. 1(a). The cutoff seen on the right-hand side of the distribution is due to the selection of $P_{lab} < 1.4$ GeV/c.

Similar distributions for all π^+ and π^- tracks are shown in Figs. 1(b,c) respectively. The kinematic cutoff at low x corresponding to $P_{lab} < 1.4$ GeV/c is again seen in both plots. The remarkably different properties of pion and proton distributions are also apparent.

Before discussing the detailed properties of these distributions, we note that this data complements existing ISR data because first round, single-particle ISR experiments have not explored the smallest angular region possible. This is illustrated by Fig. 2 (reproduced from the talk by J. C. Sens at the 1972 Oxford Conference). Lines for pions and protons with $P_{lab} = 1.4$ GeV/c are superimposed. Our data explore the regions to the right of these curves with no further acceptance corrections necessary.

In Fig. 3 we demonstrate how the bubble-chamber data complements the ISR data with a comparison between inclusive proton spectra of the CERN-Holland-Lancaster-Manchester[2] collaboration at $\sqrt{s} = 23.6$, 30.8, and 44.6, respectively. The overall normalization agreement between the two sets of data is quite good as seen in the region of overlap. The bubble-chamber data extends to lower values of P_t than the ISR data. Although the ISR data points in themselves represent a rather impressive test of scaling over the P_t and energy ranges they represent, they cutoff at $P_t = 0.5$ GeV/c and thus our data at lower P_t values can only be compared with the lower energy data from BNL and CERN.[3]

Figure 4 contains more detailed comparisons between the P_t^2 dependencies of $Ed^3\sigma/dp^3$ for protons at several different values of $\bar{x}$. The essential point of these plots is to illustrate the lack of $e^{-aP_t^2}$ behavior over the entire range of P_t^2. The straight lines are those fit by Albrow et al.[4] to their own data and our invariably much lower than the small P_t^2 data. With the exception of the lowest x value of 0.45, we observe that the 300-GeV data points are in good agreement with the 24 GeV/c data of Allaby et al.[5] for $P_t^2 \lesssim 0.5\ (\mathrm{GeV/c})^2$. The relationship is more clearly displayed in Fig. 5 which compares the x-dependence of the invariant cross section $Ed^3\sigma/dp^3$ at a mean value of $P_t^2 = 0.04\ (\mathrm{GeV/c})^2$ with the Allaby et al. data. While the low- and high-energy data are in reasonably good agreement, they suggest that scaling is approached from above (i.e., lower-momenta data are larger).

In contrast to the proton data, our pion data more nearly cover the same x-P_t range as existing ISR data and thus do not add anything essentially new to the scaling comparisons made between ISR and lower energy data. However, as illustrated in Fig. 2, there is not a complete overlap; furthermore, most ISR data used for scaling comparisons is not at the lowest end of the energy range. Thus, our 300-GeV data ($\sqrt{s} = 23.9$ GeV) are of some interest.

Figures 6 and 7 display the x-dependence of the invariant cross section for π^+ and π^-, respectively, at $P_t^2 = 0.04$ and $0.16\ (\mathrm{GeV/c})^2$. In each case, scaling is seen to break down at small x for $P_t^2 = 0.04\ (GeV/c)^2$. Figures 8 and 9 display the dependences on P_t^2 at $\bar{x} = 0.21$, also for π^+ and π^-, respectively. Generally good agreement is observed, although there seems to be differences among the lowest energy data themselves.

REFERENCES

*Supported by the U. S. National Science Foundation under Grant GP-33565.

[1] F. T. Dao et al., Phys. Rev. Letters 30, 34 (1973).

[2] J. C. Sens, private communication.

[3] W. H. Sims et al., Nucl. Phys. B41, 317 (1972) and J. V. Allaby et al., contribution to the IV International Conference on High Energy Collisions, Oxford (1972).

[4] M. J. Albrow et al., contributions to the XVI International Conference on High Energy Physics, Batavia (1972) and unpublished.

[5] See Ref. 3.

FIGURE CAPTIONS

Fig. 1. Single particle $x\text{-}P_t^2$ distributions for all protons, π^+, and π^- in a sample of 1750 events. The sharp cutoffs seen at the right-hand edge of each distribution are due to the 1.4 GeV/c laboratory momentum cutoff imposed in the measurements.

Fig. 2. Illustration of how present data complements existing ISR data for single-particle inclusive reactions.

Fig. 3. P_t distribution for protons at a mean $\bar{x} = 0.8$. The bubble-chamber data are averaged over the range x = 0.7 to 0.9, and are compared with the ISR data of the CERN-Holland-Lancaster-Manchester collaboration of Albrow et al.

Fig. 4. P_t^2 distributions for protons at $\bar{x} = 0.45$, 0.55, 0.65, 0.75, and 0.825. This data is compared with the ISR data of Albrow et al. and the 24 GeV/c data of Allaby et al.

Fig. 5. x distributions of protons for $P_t^2 = 0.04$ (0.02 - 0.06) compared to Allaby et al. data.

Fig. 6. x distributions of π^+ for $P_t^2 = 0.04$ and 0.16 GeV^2. The data is compared to the ISR data and low-energy Panvini et al. and Allaby et al. data.

Fig. 7. x distributions of π^- for $P_t^2 = 0.04$ and 0.16 GeV^2.

Fig. 8. P_t^2 distributions of π^+ for $\bar{x} = 0.21$.

Fig. 9. P_t^2 distributions of π^- for $\bar{x} = 0.21$.

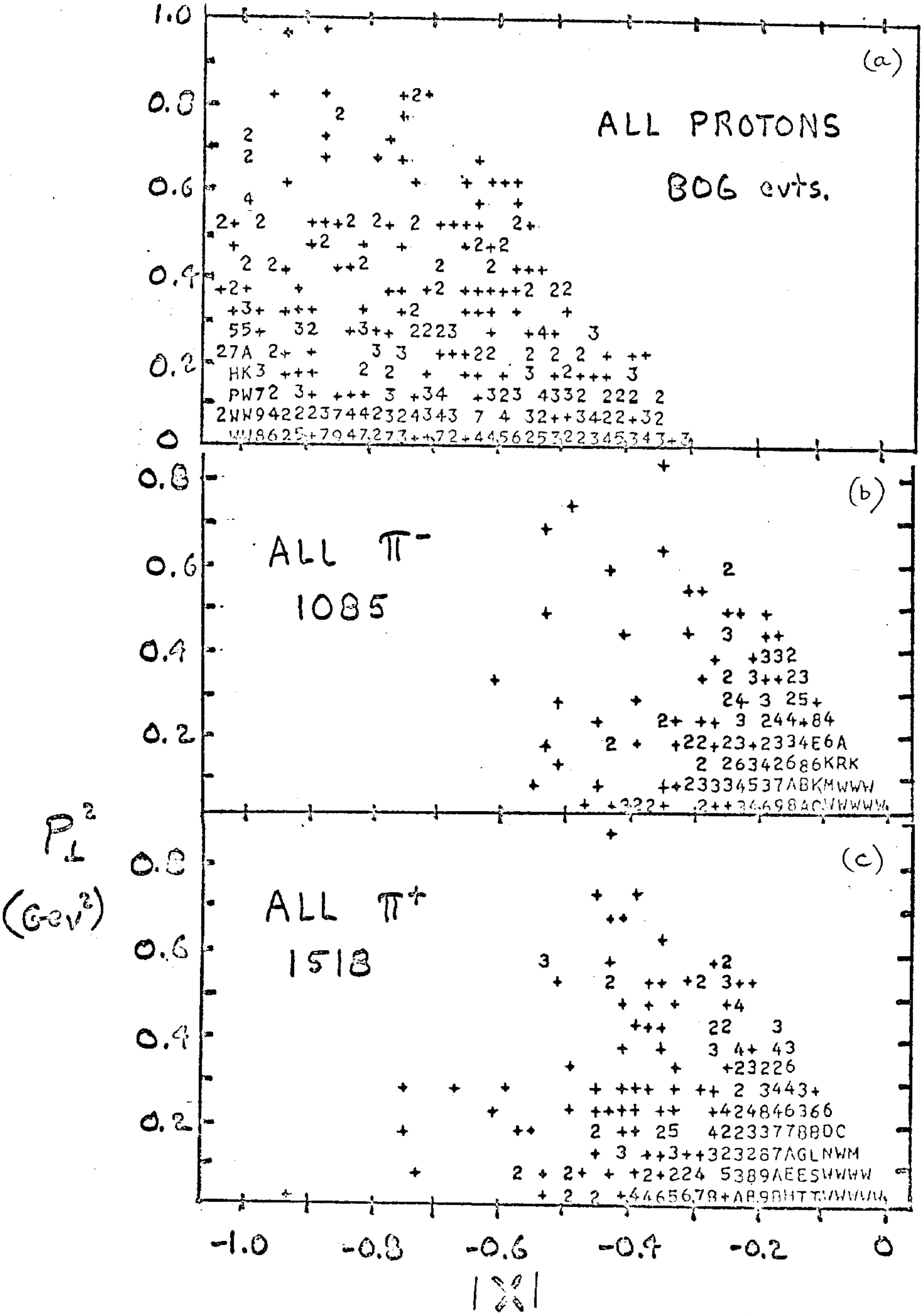
(a)
ALL PROTONS
806 evts.
(b)
ALL π⁻
1085
(c)
ALL π⁺
1518
1.0
0.8
0.6
0.4
0.2
0
-1.0
-0.8
-0.6
-0.4
-0.2
0
P⊥² (GeV²)
|x|

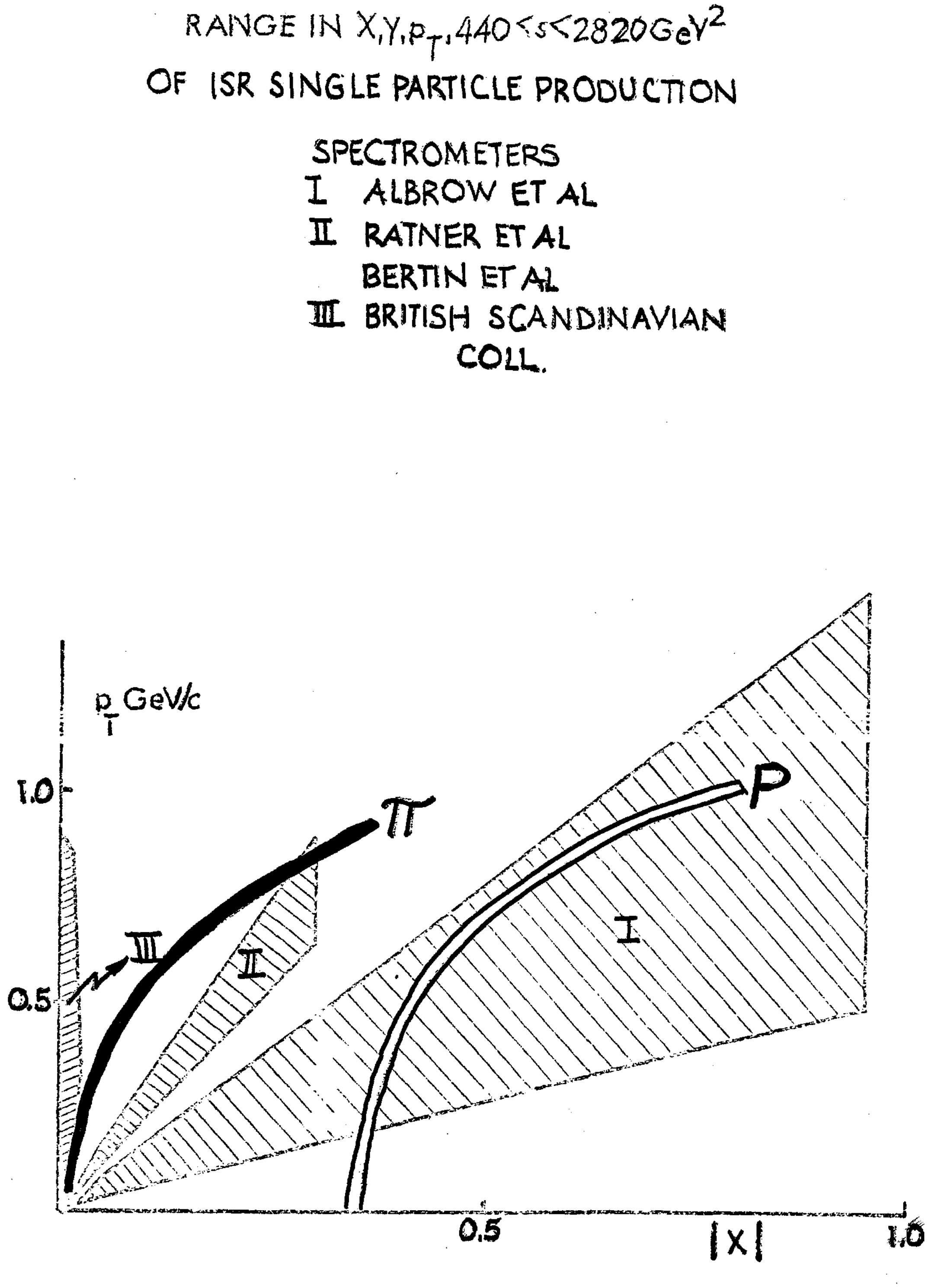

Fig. 2

(From invited talk by J. C. Sens at 1972 Oxford Conference.)

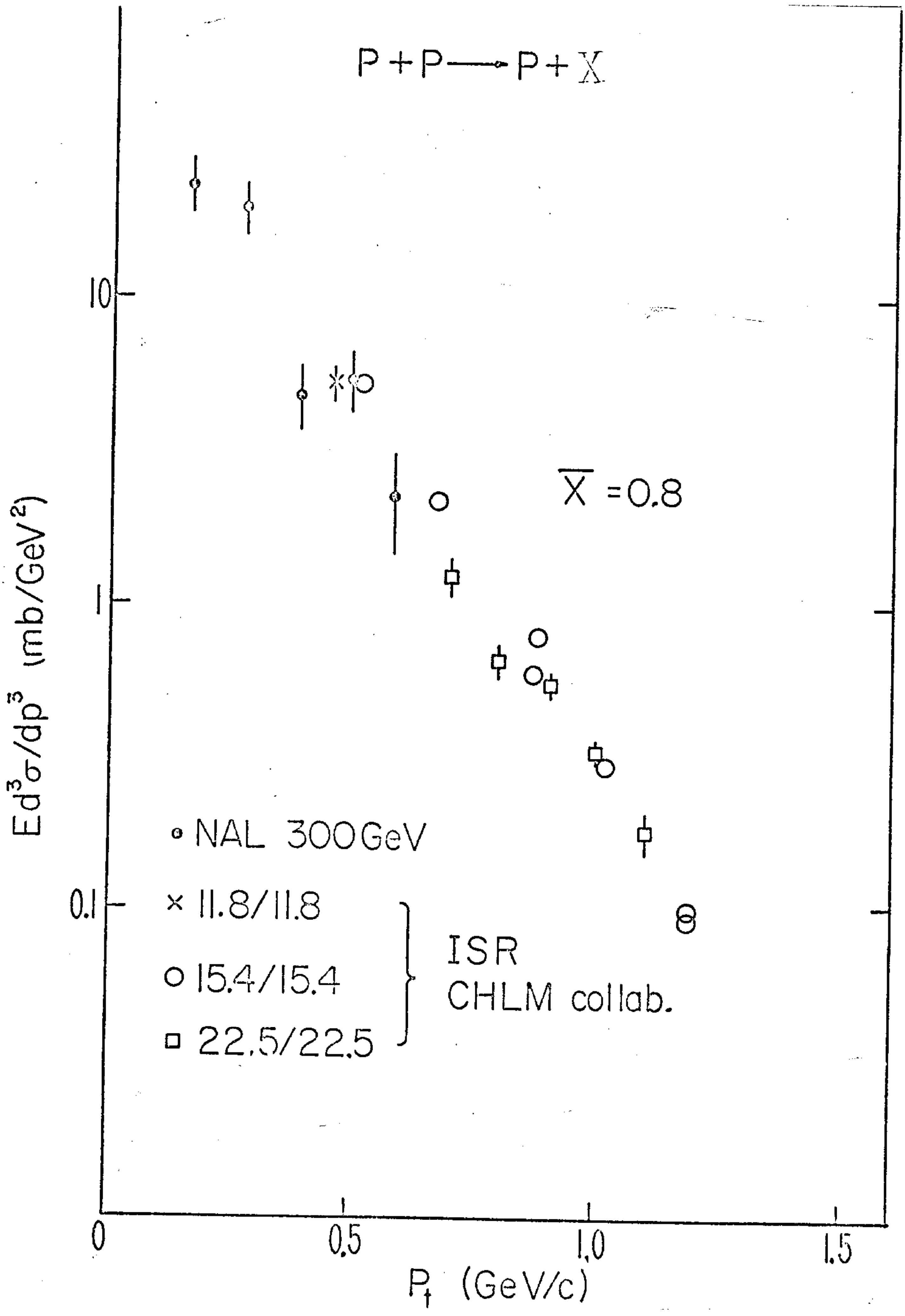

P + P → P + X
$\overline{X}$ = 0.8
10
1
0.1
0
0.5
1.0
1.5
$Ed^3\sigma/dp^3$ (mb/GeV^2)
P_t (GeV/c)
NAL 300 GeV
11.8/11.8
15.4/15.4
22.5/22.5
ISR
CHLM collab.

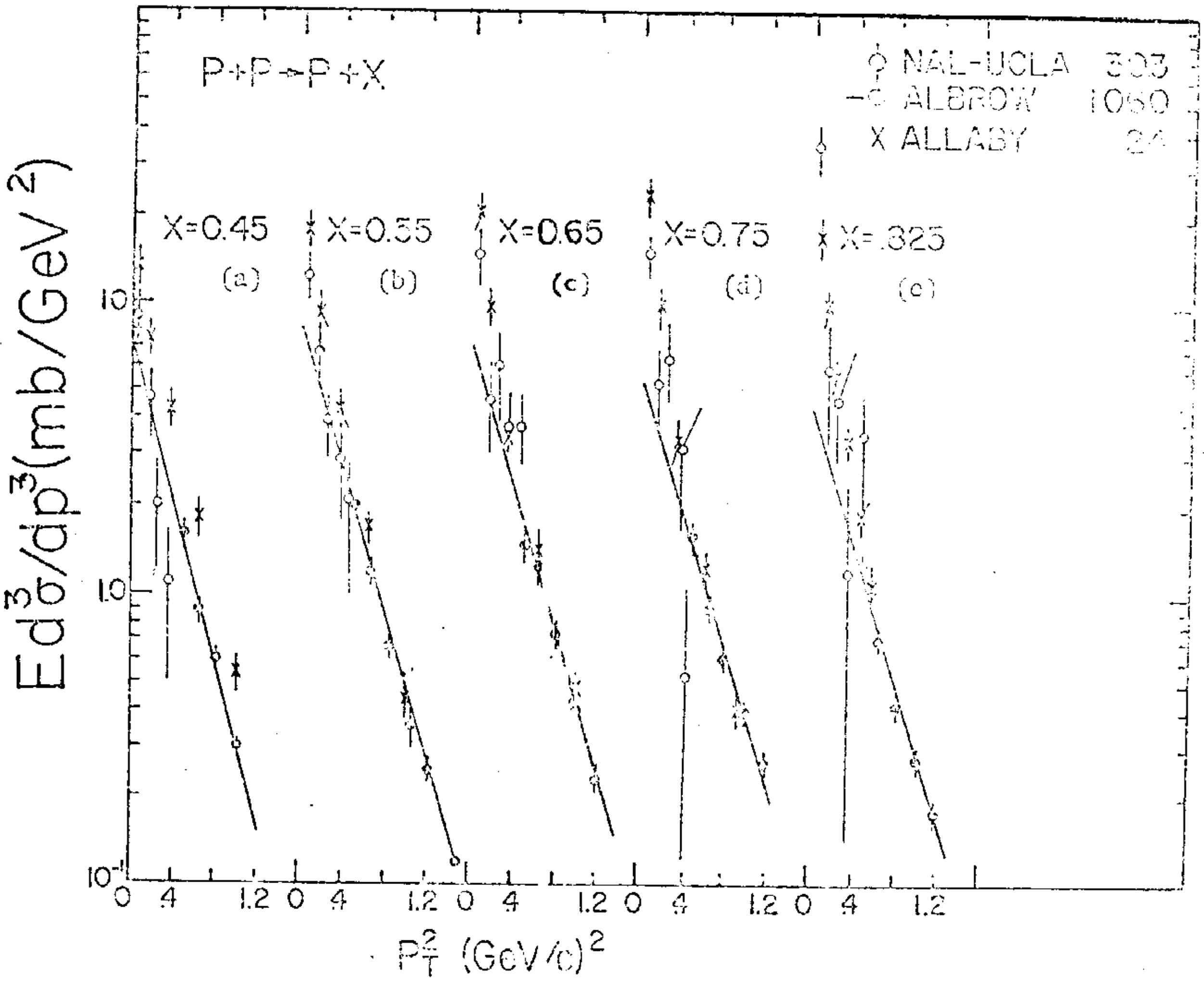
P+P→P+X
NAL-UCLA 303
ALBROW 1060
X ALLABY 24
X=0.45
(a)
X=0.55
(b)
X=0.65
(c)
X=0.75
(d)
X=.325
(e)
10
1.0
10⁻¹
0
4
1.2
$Ed^3\sigma/dp^3$(mb/GeV ^{2})
P_T^2 (GeV/c)^2

Fig. 4

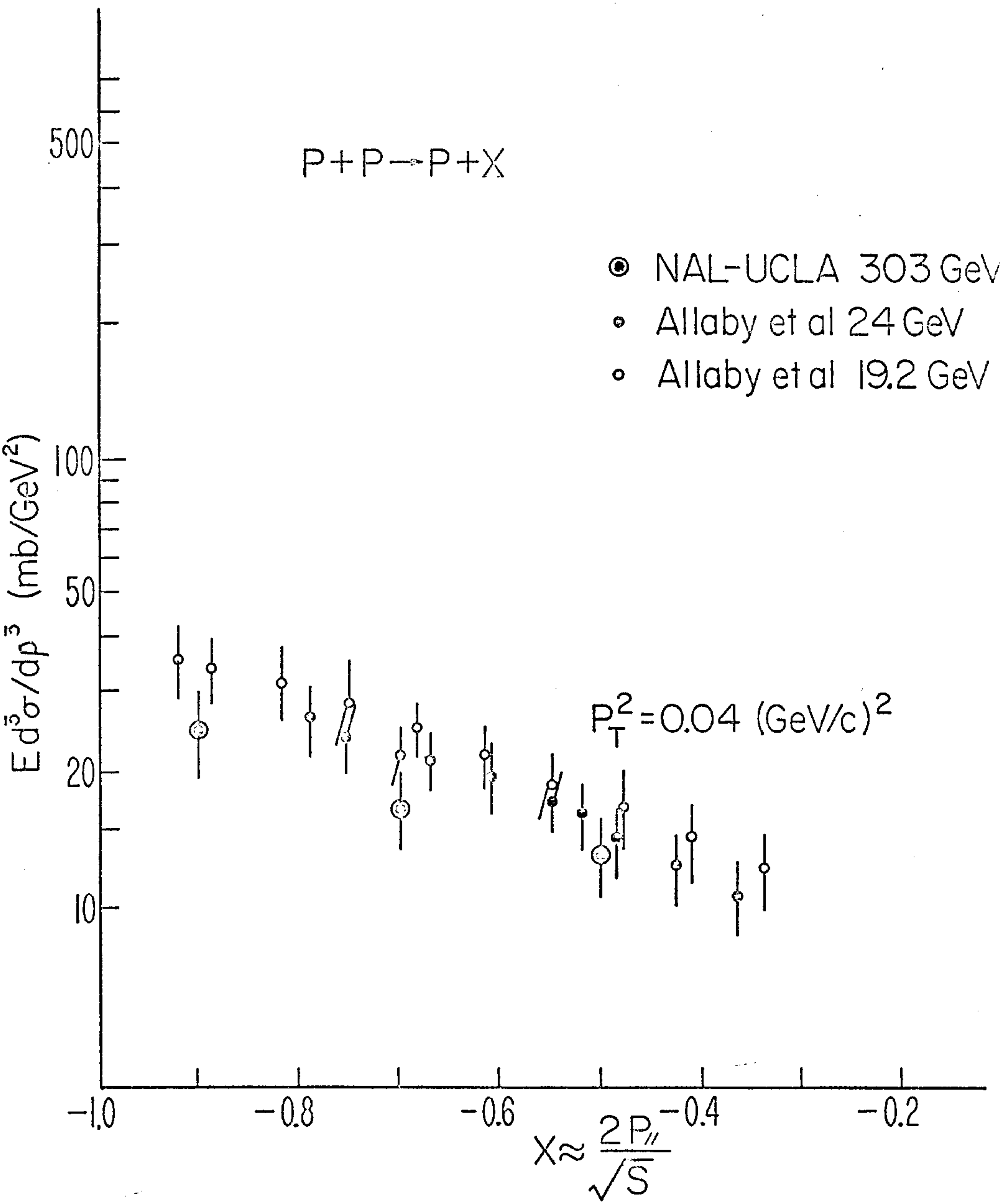
P+P→P+X
NAL-UCLA 303 GeV
Allaby et al 24 GeV
Allaby et al 19.2 GeV
$P_T^2 = 0.04\ (GeV/c)^2$
$E d^3\sigma/dp^3$ (mb/GeV^2)
500
100
50
20
10
−1.0
−0.8
−0.6
−0.4
−0.2
$X \approx \frac{2P_{\parallel}}{\sqrt{S}}$

Fig. 5

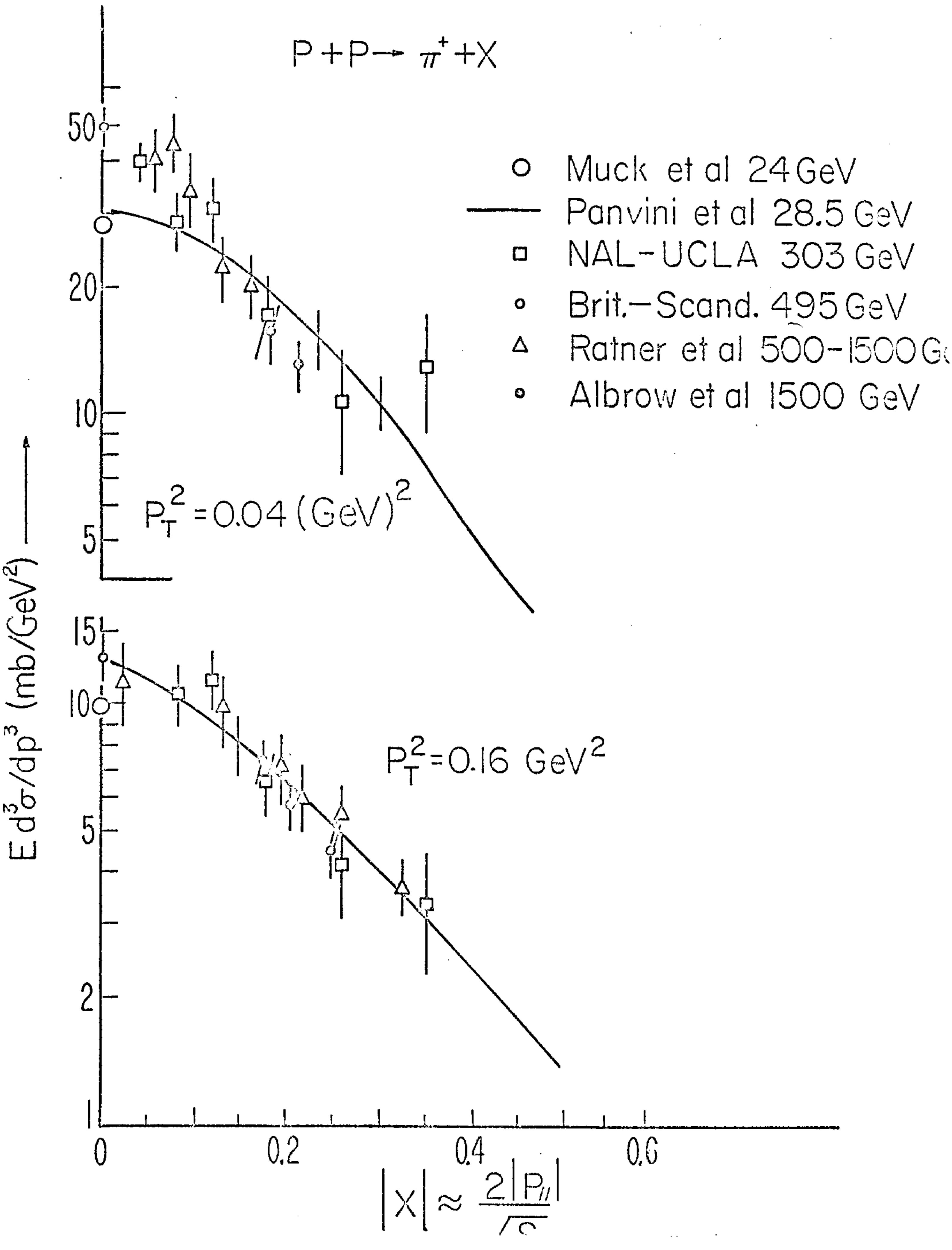

P + P → π⁺ + X
Muck et al 24 GeV
Panvini et al 28.5 GeV
NAL-UCLA 303 GeV
Brit.-Scand. 495 GeV
Ratner et al 500-1500 G
Albrow et al 1500 GeV
$P_T^2 = 0.04\ (GeV)^2$
$P_T^2 = 0.16\ GeV^2$
$E\,d^3\sigma/dp^3$ (mb/GeV²)
50
20
10
5
15
10
5
2
1
0
0.2
0.4
0.6
$|X| \approx \frac{2|P_{//}|}{\sqrt{s}}$

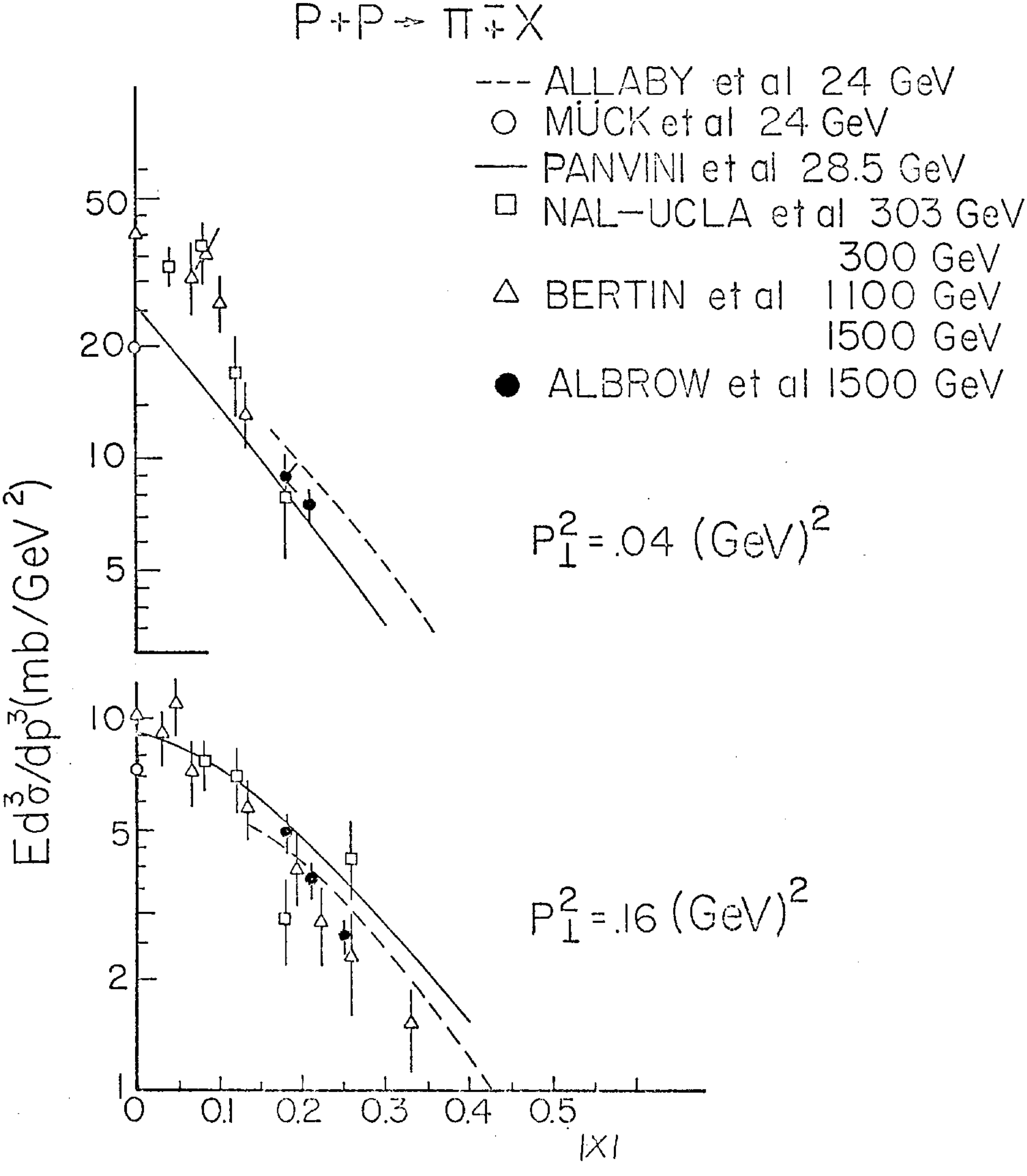
P+P → π∓X
--- ALLABY et al 24 GeV
○ MÜCK et al 24 GeV
— PANVINI et al 28.5 GeV
□ NAL-UCLA et al 303 GeV
300 GeV
△ BERTIN et al 1100 GeV
1500 GeV
● ALBROW et al 1500 GeV
$P_\perp^2 = .04\ (GeV)^2$
$P_\perp^2 = .16\ (GeV)^2$
$Ed^3\sigma/dp^3$ (mb/GeV^2)
50
20
10
5
10
5
2
1
0
0.1
0.2
0.3
0.4
0.5
|X|

Fig. 7

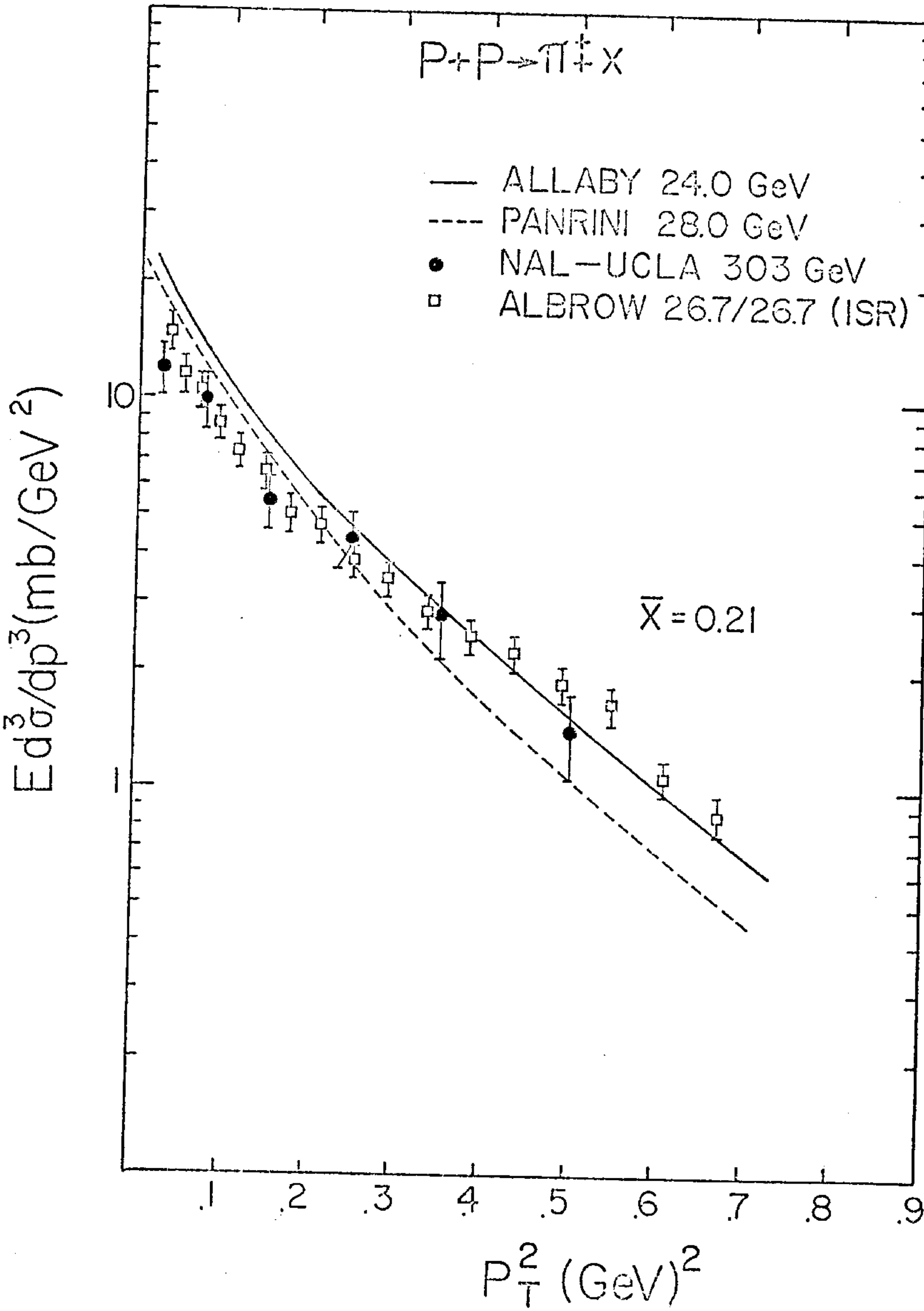
P+P→π±X
ALLABY 24.0 GeV
PANRINI 28.0 GeV
NAL—UCLA 303 GeV
ALBROW 26.7/26.7 (ISR)
X̄ = 0.21
10
1
.1
.2
.3
.4
.5
.6
.7
.8
.9
Edσ³/dp³(mb/GeV²)
P²T (GeV)²

Fig. 8

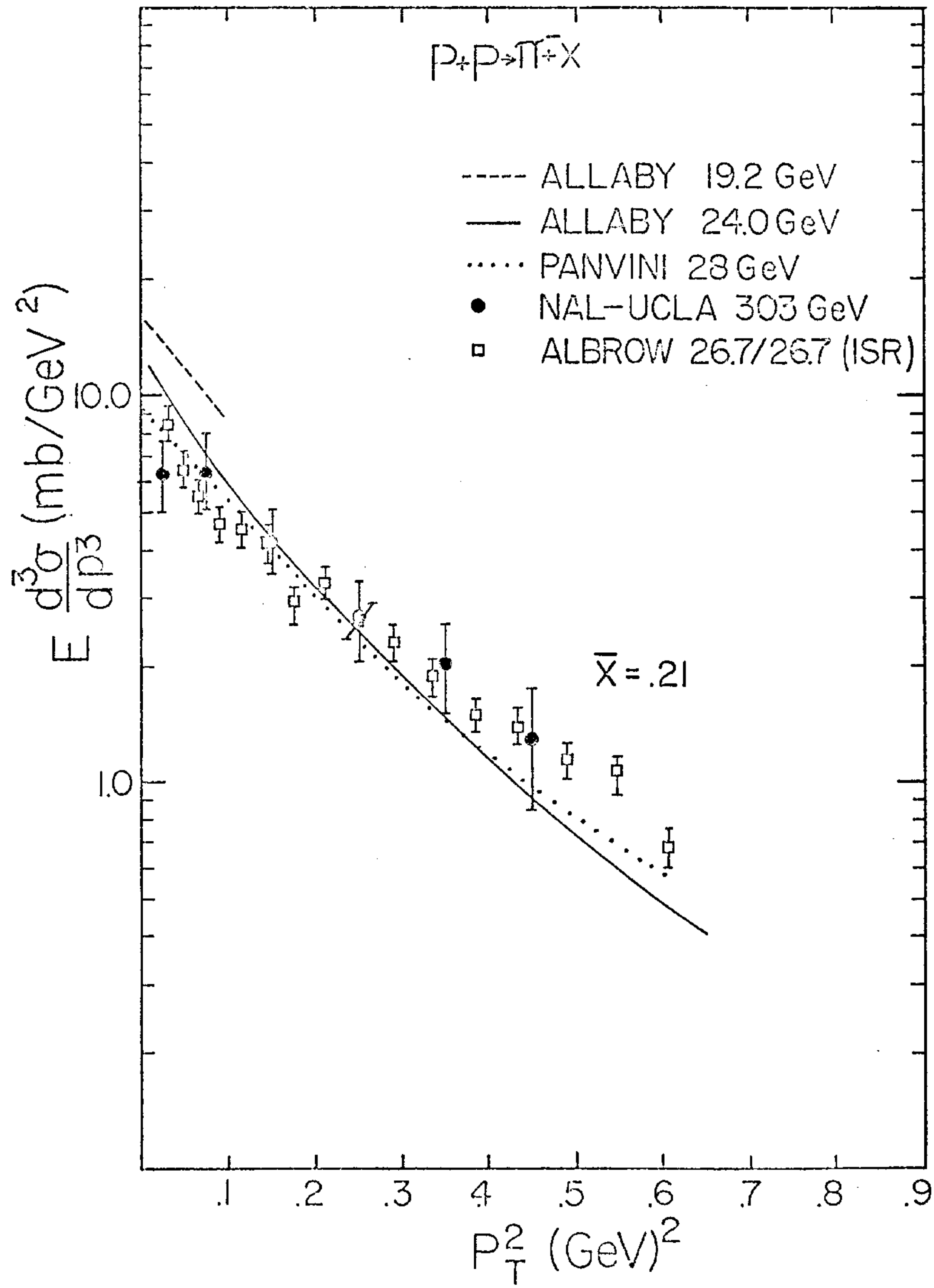

P+P→π⁻+X
----- ALLABY 19.2 GeV
—— ALLABY 24.0 GeV
····· PANVINI 28 GeV
● NAL-UCLA 303 GeV
□ ALBROW 26.7/26.7 (ISR)
$\bar{X}$ = .21
10.0
1.0
$E \frac{d^3\sigma}{dp^3}$ (mb/GeV^2)
.1
.2
.3
.4
.5
.6
.7
.8
.9
P_T^2 (GeV)^2

Fig. 9